10th International Conference
12-14 July 2010
Southampton
RASD 2010

MODEL UNCERTAINTY IN IDENTIFICATION OF THE STATIC CHARACTERISTICS OF THE HYDRAULIC DAMPER

Branislav Titurus[1*], Jonathan du Bois[1], Nick Lieven[1], Robert Hansford[2]

[1] Department of Aerospace Engineering, University of Bristol, Queens Building, University Walk, Bristol, BS8 1TR, UK

[2] Box 267, Westland Helicopters, Lysander Road, Yeovil, Somerset, U.K.

Keywords: hydraulic damper, model uncertainty, identification, static characteristics

ABSTRACT

The research presented in the current paper focuses on the analysis of the model uncertainty in the static part of hydraulic damper models. Recently established experimental and identification methodology provides non-parametric estimates of the overall static characteristics of velocity-sensitive hydraulic dampers. Previously identified non-parametric static characteristics of a helicopter hydraulic damper are investigated in this paper. A model uncertainty is presented in the form of two alternative pressure-flow models that are considered herein. The main goal of this paper is to assess the feasibility of a non-parametric static representation of the damper in its ability to indicate the actual fluid flow topology and the flow regimes established by the experimental conditions.

1. INTRODUCTION

There exists a broad class of hydraulic devices employing force generation mechanisms resulting from restricted flow conditions. These devices are frequently used in technological areas such as car suspensions, building seismic protection and helicopter rotor stability. Precise mathematical physically-based models of these devices are obvious and often the key components in a range of analyses performed during the component life cycle. However, a wide spectrum of physical conditions in the dampers requires increased attention during modelling.

A recently developed experimental technique, presented in [1], is used here to provide a basis for mathematical model structure investigations of a hydraulic damper. The main feature of this technique is the use of a triangular waveform piston excitation that imposes a

quasi-steady flow condition in the investigated system. An identical form of piston excitation was applied for the damper investigation in [2]. The application of these conditions in the damper provides a precise and focused tool for non-parametric identification of the overall static characteristics of symmetric, velocity sensitive hydraulic dampers. The damper model derived in [3] can be used to model this type of hydraulic damping device. As presented in paper [1] the technique allows the identification of the static part of the model.

However, any further progress in parameter-based modelling requires assumptions about the topology of the paths that are responsible for the observed pressure losses. While different damper designs are characterised by different internal organisation of the flow passages, there also exists a degree of uncertainty with regards to how other, nominally closed links contribute to the system behaviour and its characteristics. This uncertainty is often associated with the sources of cross-chamber leakage and the relative contributions of laminar and turbulent flow to the pressure losses. The effect of uncertain flow conditions can be observed on the hydraulic component level [4], while topological uncertainty can be related to non-ideal seals and fittings located between the two working chambers of the damper. To address this problem on the overall damper level two alternative assumptions are often made. In the first case a combination of laminar and turbulent pressure losses are associated with the primary flow path, modelled as a serial arrangement of laminar and turbulent pressure loss restrictors as documented for example in [6] and [7]. Alternatively, the primary flow path is assumed to consist purely of turbulent losses, while laminar losses are associated with parallel flow branches, often present due to leakage flows between chambers as documented for example in [8] and [9]. Further, parallel arrangements of the laminar and turbulent loss features are often used in models of linear hydraulic actuators, e.g. [10].

The goal of this paper is to analyse the feasibility of objective identification of the "correct" flow mechanism based on the overall static characteristics of the damper. This study is based on data acquired from tests on a symmetric hydraulic damper with through rod, used in the aerospace sector for stability augmentation purposes. The first part of the paper introduces the theoretical concepts and experimental methodology employed in the non-parametric damper identification. The second part of the paper presents an actual case study and an analysis of the results.

2. BUILDING BLOCKS OF THE EVALUATION METHODOLOGY

2.1 Damper mathematical model and its static characteristics

The type of device considered in this paper is a symmetric hydraulic damper with through rod. An example of this damper is presented in Figure 1. The solid arrow denotes the nominal flow path, while dashed arrows represent flow paths potentially present due to cross-flow and leakage. This can happen between moving surfaces, due to non-ideal or worn seals located between working chambers of the damper and due to non-ideal behaviour of valves.

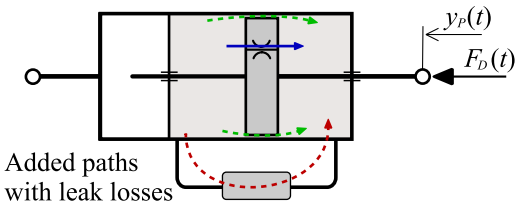

Figure 1 Baseline damper arrangement.

The model suitable for the analysis of these devices is derived in [1] and it can be written in the following form

$$\begin{gathered}\beta_{eff}\mathcal{V}(y_p)\Delta\dot{p}+Q_N(\Delta p)=A_P\,\dot{y}_P,\\ \mathcal{V}(y_p)=V_1V_2/(V_1+V_2),\ V_1(y_p)=V_{0,1}-A_Py_P,\ V_2(y_p)=V_{0,2}+A_Py_P\end{gathered}\tag{1}$$

where the term $Q_P=A_P\,\dot{y}_P$ represents the flow rate induced by the movement of the piston with a cross-sectional area A_P and a velocity $\dot{y}_P$, $Q_N=\sum_{(k)}Q_k$ is the total flow rate between the damper chambers represented as a sum of contributions Q_k from individual flow paths, the term $Q_\beta=\beta\,\mathcal{V}(y_p)\Delta\dot{p}$ represents the induced flow rate due to effective fluid compressibility and $V_i, V_{0,i}$ are the i-th variable and initial volumes of the chambers, respectively.

The total flow rate between the damper chambers, Q_N, determines to a significant extent the behaviour of the damper and can be seen as an overall static characteristic of the device, or alternatively it can be seen as part of the model of the damper for an idealized situation with an incompressible working fluid. Assuming an incompressible configuration with $\beta=0$ in model (1) and the existence of an inverse function $Q_N^{-1}(\circ)$, the following can be taken as the overall static characteristics of the damper

$$\begin{gathered}\Delta p=Q_N^{-1}(Q_P)\equiv P(Q_P),\\ F_D\approx A_P\,Q_N^{-1}(A_P\,\dot{y}_P)\equiv F(\dot{y}_P).\end{gathered}\tag{2}$$

The approximate equality in the previous formula indicates the fact that any damper force will be affected to a certain extent by other unaccounted physical interactions such as mechanical friction. The ability to observe the quantities presented in equation (2) therefore forms one step in the determination of the essential components of model (1) and it motivates the experimental methodology employed in this paper.

2.2 Damper flow networks

The total flow between the working chambers of the damper is determined by the resistive nature of the flow passages located between them, as well as by the topology of this flow network. Moreover, this network can be of variable structure achieved either by passive (flow dependent components such as check valves, relief valves etc.) or active means (solenoid valves, direct drive continuous valves etc.).

In this paper the basic mechanisms of the pressure losses are considered to be caused by idealised laminar and turbulent flow conditions in the form of discrete pressure loss elements. These mechanisms are considered as these are particularly relevant to the steady flow conditions that will be later imposed by the testing methodology. The components of the hydraulic networks are therefore laminar and turbulent loss flow restrictors in parallel and serial arrangements. The static characteristics of individual elements are assumed to take the form $\Delta p_L=C_L\,Q$ for the laminar losses and $\Delta p_Q=C_Q\,Q|Q|$ for the turbulent losses with the coefficients C_L and C_Q constituting an amalgamation of the relevant physical parameters [1].

The assumption of incompressible fluid allows conversion of the standard compressible hydraulic system equation for the general i-th volume [5] into a form suitable for identification of the static characteristic

$$\beta_i(p_i)V_i\,\dot{p}_i+\dot{V}_i=\sum_{(j)}Q_{i,j}(\Delta p_{i,j})\rightarrow\dot{V}_i=\sum_{(j)}Q_{i,j}(\Delta p_{i,j}),\ i=1,\ldots,N_V \tag{3}$$

where $Q_{i,j}$ is the flow rate between the i-th and j-th fluid volumes (nodes) with their associated pressure difference $\Delta p_{i,j}=p_i-p_j$. In this sense the relationship in (3) constitutes a system of N_V algebraic equations for an equal number of nodal pressures p_i such that flow rate equilibrium in the system is established. The problem (3) can be therefore written in the generic mathematical form

$$\mathbf{g}(p_1,p_2,\ldots,p_{N_V};y_P,\dot{y}_P,\mathbf{p})=\mathbf{0} \tag{4}$$

where p_i are the unknown pressures, y_P and $\dot{y}_P$ are the prescribed piston displacement and velocity, respectively, and $\mathbf{p}\in\mathbb{R}^{N_P}$ is the vector of N_P physical parameters of the model.

In the context of a system designed to dissipate mechanical energy, it is the pressure difference between the two specific nodal points that is responsible for the induced net resistive mechanical force, e.g. $F_D\approx A_P\,\Delta p_{1,2}$. This approach allows "static" parameter identification in the context of steady flow conditions as described later in this paper. A major benefit of this method is that it allows direct conversion of the system-dynamic model to its "static" form without additional modelling work.

An alternative approach can be used for the case where the unknown variables are volumetric flow rates between fluid nodes, i.e. $Q_{i,j}$. While in the first case the knowledge of the component functions $Q_{i,j}=f(\Delta p_{i,j})$ is expected during model construction, in this second approach the inverse functions $\Delta p_{i,j}=f^{-1}(Q_{i,j})$ are required during the model building stage. In this paper both approaches will be used to formulate problem descriptions suitable for parameter identification based on measured data.

2.3 Experimental methodology for nonparametric identification

The experimental methodology used in this paper is based on imposing quasi-steady flow conditions in the hydraulic damper. For this purpose, a so called iso-kinetic excitation [2] is used. The experimental methodology is formalized in [1] while the first use of the iso-kinetic excitation was presented in [2]. This method allows detailed non-parametric mapping of the damper static characteristics. The iso-kinetic excitation is represented by a triangular piston displacement motion.

The use of this type of excitation leads to a piece-wise constant velocity $\dot{y}_P=\pm W_P$ being applied to the damper piston, thus introducing a constant prescribed flow rate $Q_P=A_P W_P$. The application of this assumption in model (1) introduces a step excitation with initial transients followed by stabilization to the quasi-steady operational conditions. In the practical context this stage is used to acquire the data used for non-parametric static characteristic identification. A detailed description of the methodology along with an analysis of the quasi-steadiness is provided in [1]. A specific example of the identified characteristics along with

selected underlying signals is provided in the following case study section.

3. CASE STUDY

3.1 Identified nonparametric static damper representation

The identification experiment was conducted on a hydraulic damper used in rotorcraft for stability purposes [1]. The purpose of the experiment was to identify the static characteristics of this damper in the low velocity range, less then $2\,mm/s$, where its performance is primarily determined by a single fixed orifice located in the piston head. This technique was considered to be suitable due to its ability to avoid limitations associated with standard harmonic piston excitation based identification techniques such as unwanted compressibility effects, mechanical backlash etc. Further, a useful feature of this technique is its ability to focus on the ranges of very low piston velocity excitations that are normally dominated by non-hydraulic effects.

The basic outline of the experimental setup is described in Figure 2a) and the outline of the relevant parts of the damper is presented in Figure 2b). Despite the fact that the actual damper has a more complex structure, the intention of the study presented here was to describe only the orifice-driven overall characteristics of the damper. A set of alternative flow paths is also shown as grey lines in Figure 2b). Experimental parameters were defined such that the conditions for the activations of these paths were not achieved throughout the tests.

The test system was based on the combination of Instron and dSpace platforms with one control channel supplying the prescribed piston displacement signal and two measured output signals – the displacement of the actuator piston via an integrated LVDT and the force in the serial damper-actuator arrangement via a load cell located between the damper and the actuator.

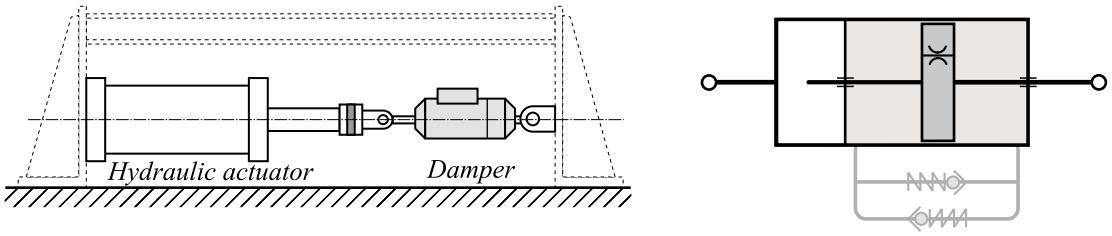

a) b)

Figure 2 Test rig setup for the hydraulic damper:
a) test rig configuration, b) nominal structure of the damper without relief valves activated.

A set of triangular excitation runs with varying amplitude and frequency was applied to the damper to achieve predefined constant excitation velocities $\pm\dot{y}_{P,i} = v_{P,i}$, where $i = 1,\ldots,23$. The test was conducted for approximately constant temperature of $T \approx 40\,^{\circ}C$ as measured on the surface of the damper. Each run consisted of four complete linear displacement slopes resulting into two instances of the same excitation conditions in each test run, thus allowing repeatability tests. For each constant velocity excitation, i.e. each linear slope, a data subset was selected from the section with apparently steady damper response. The data subsets extracted in this way were later fitted with linear functions. These pairs of identified

responses, $[v_{P,m,i}, F_{D,m,i}]$, were used to construct the damper characteristics.

Figure 3 shows two selected test runs chosen to demonstrate low and "high" velocity excitation cases. Each subplot contains all the relevant components of the non-parametric identification. The measured piston displacement signal is scaled to allow comparison with the measured force signal. Both signals are also shown with their corresponding linear fits identifying one point of the damper characteristic curve.

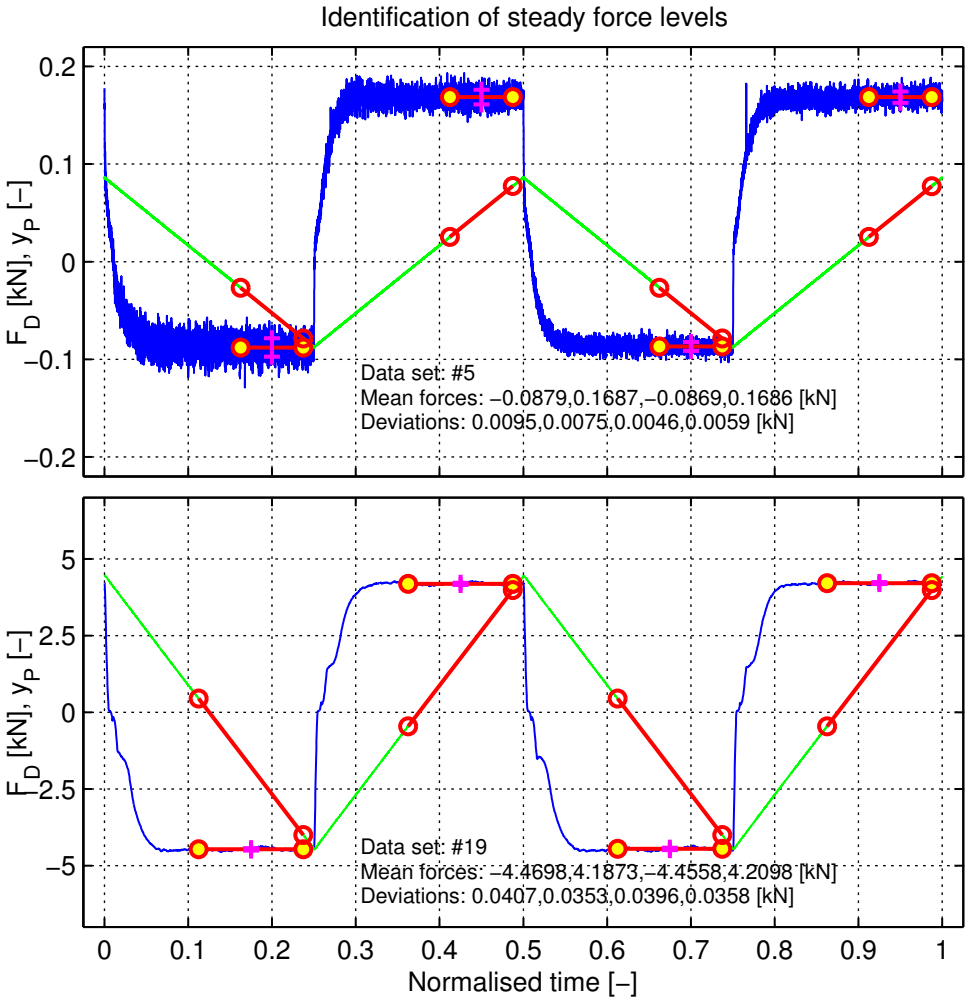

Figure 3 Examples of identification of steady force levels for two selected datasets.

A summary of all the test cases is provided in Figure 4. The damper characteristics presented in the left subplot identify damper static characteristics in the linear domain, while the right subplot shows the same data in the logarithmic domain. Evaluation of the damper characteristics in the logarithmic domain allows observation of the nature of the flow regimes and associated physical mechanism as well as their transitions with increasing piston and flow velocity. Further analysis of the test results and their relationship with standard test techniques is provided in [1].

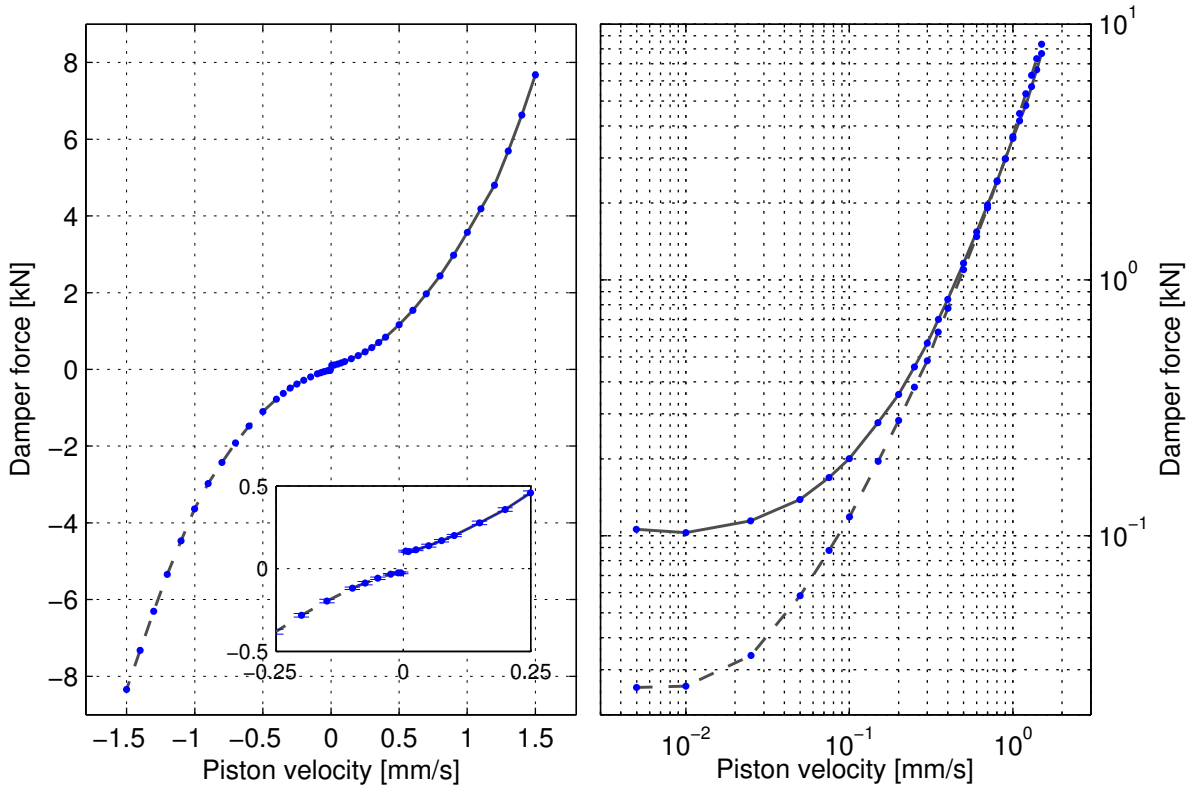

Figure 4 Identified static characteristics of the damper in linear and logarithmic scales. The dashed line represents the data from the negative quadrant of the linear plot.

3.2 Application of selected network representations

This section uses the previously identified experimental data for further considerations related to the investigation of the structure of the flow paths responsible for the pressure losses observed in the measured data. As already indicated in the section 1, two alternative representations are traditionally used to represent a combined laminar-turbulent environment in hydraulic dampers. In one case a serial arrangement of laminar and turbulent pressure loss features are considered, e.g. [6] and [7], while in the second case a parallel arrangement of laminar and turbulent pressure loss sources is considered, e.g. [8], [9] and [10]. These two alternative flow path organisations are shown in Figure 5.

The corresponding direct and inverse static characteristics of the serial laminar-turbulent network shown in Figure 5a), assuming $\Delta p, Q \geq 0$, is specified as follows

$$\Delta p = C_{S,L}\, Q + C_{S,Q}\, Q^2, \;\; Q = \frac{-C_{S,L} + \sqrt{C_{S,L}^2 + 4\, C_{S,Q}\, \Delta p}}{2\, C_{S,Q}} \tag{5}$$

and the same functions specified for the parallel laminar-turbulent network shown in Figure 5b), assuming $\Delta p, Q \geq 0$, is written in the form

$$Q = C_{P,L}^{-1}\,\Delta p + C_{P,Q}^{-1}\sqrt{\Delta p}\,,\;\; \Delta p = \frac{C_{P,Q}^{-2} + 2\,C_{P,L}^{-1}\,Q - \sqrt{C_{P,Q}^{-4} + 4\,C_{P,L}^{-1}\,C_{P,Q}^{-2}\,Q}}{2\,C_{P,L}^{-2}} \tag{6}$$

where, based on Figure 5b), the overall coefficient corresponding to the laminar flow branches is defined as $C_{P,L} = \sum_{(j)} C_{P,L\,j}$.

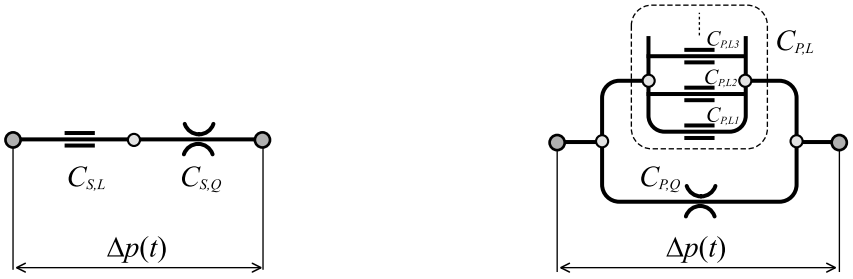

Figure 5 Two alternative flow networks considered for parametric identification: a) serial laminar-turbulent arrangement, b) parallel laminar-turbulent arrangement.

While equations and are expressed in terms of pressure differentials, flow rates and their corresponding parameters, in accordance with the theoretical development in section 2, the experimental data and resulting characteristics are presented in terms of overall damper forces and piston velocities. The transformation relationships can be established between these two sets of quantities in the form $F_D \approx A_P\,\Delta p$ and $Q \approx Q_P = A_P\,\dot{y}_P$. The validity of these relationships and their approximate nature are discussed in [1]. Further, as already shown in Figure 4, the data in the velocity-force domain are scaled to a set of units more suitable for least squares-based identification. Considering equations and and the aforementioned transformations between the pressure-flow and velocity-force domains, i.e. Figure 4, a relationship can be established between coefficients $C_{\circ,L}$ and $C_{\circ,Q}$ and the coefficients obtained from the identification performed on the data shown in Figure 4. As this transformation contains a commercially sensitive parameter A_P , all subsequent activities will be performed directly on velocity-force data as presented in Figure 4.

Equations and are used as a suitable basis for parametric identification of the static characteristics as presented in Figure 4. A linear least square identification problem for the case of the serial laminar-turbulent arrangement, Figure 5a), is based on following equation written for the i-th identified point of the characteristics

$$\begin{bmatrix} Q_i & Q_i^2 \end{bmatrix} \begin{bmatrix} C_{S,L} \\ C_{S,Q} \end{bmatrix} = \Delta p_i,\;\; i = 1,\ldots,N_{ID}. \tag{7}$$

A similar linear least square formulation can be applied to the case of the parallel laminar-turbulent arrangement, Figure 5b), and the i-th identified point of the characteristics

$$\begin{bmatrix} \Delta p_i & \sqrt{\Delta p_i} \end{bmatrix} \begin{bmatrix} C_{P,L}^{-1} \\ C_{P,Q}^{-1} \end{bmatrix} = Q_i,\;\; i = 1,\ldots,N_{ID}. \tag{8}$$

In equations (7) and (8) the parameter $N_{ID} \leq 23$. The resulting problem will have the standard form $\mathbf{A}\mathbf{x}=\mathbf{b}$, with the assembled matrix $\mathbf{A} \in \mathbb{R}^{N_{ID} \times 2}$ and the corresponding vectors $\mathbf{x}, \mathbf{b} \in \mathbb{R}^{N_{ID}}$ being dependent on the specific forms of (7) and (8). The coefficient vector is determined via $\mathbf{x}=\mathbf{A}^{+}\mathbf{b}$, where $\mathbf{A}^{+}$ is the matrix pseudo-inverse.

There are two further pre-processing steps applied to the data shown in Figure 4. The first step involves the selection of data corresponding to quadrant 1, i.e. $F_{D,i}, \dot{y}_{P,i} \geq 0$. This selection facilitates the identification of the losses corresponding to a single flow direction. This step is relevant in the cases of asymmetric flow restrictors or networks consisting of these components. As can be observed in Figure 4b) this is the case in the current study. The application of this experimental methodology can detect asymmetric effects and it allows the assessment of their significance. The second step in the data pre-processing is the removal of the offset from data on the vertical axis of Figure 4. This offset has origins in non-fluidic interactions such as friction. In the present case the effect of the friction is assumed to be approximately constant for the piston speeds considered and the value $F_{D,offset}=\min([F_{D,i}])$, $i=1,\ldots,23$ is used to modify the data such that $\tilde{F}_{D,i}=F_{D,i}-F_{D,offset}$. The data pairs $[\dot{y}_{P,i}, \tilde{F}_{D,i}]$ are used in this case study for the actual parametric identification. The results of the identification are shown in Figure 6 and Figure 7.

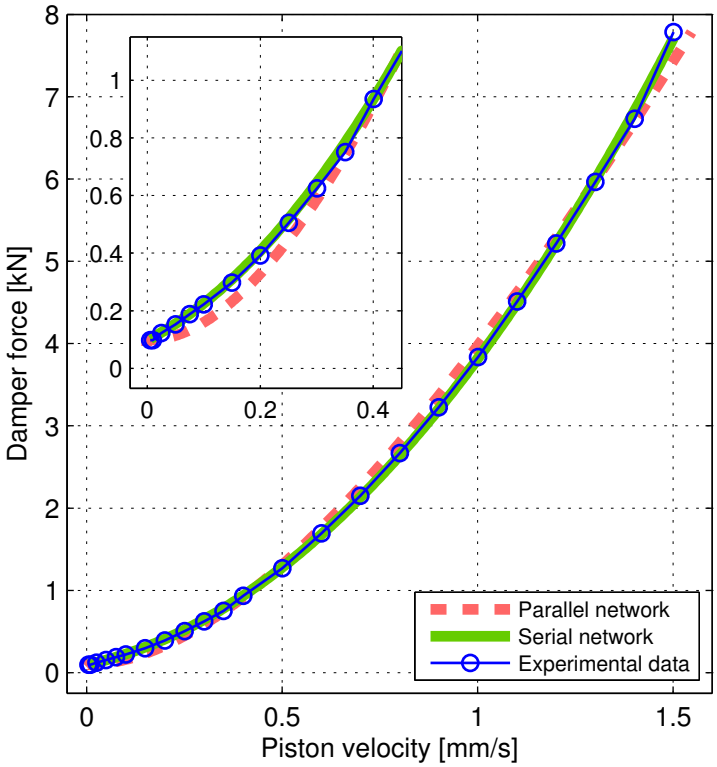

Figure 6 Comparison of identified parametric models with experimental data using linear scales.

In the present study 21 data points were used to assemble the equations, where the first two points (corresponding to the lowest piston velocities) were not included in the identification due to being significantly affected by mechanical friction. Figure 6 compares experimental

and analytical data using linear scales. This comparison documents the overall performance of the network representations in modelling the data. The results presented suggest that for the current case the parallel network model is outperformed by that of the serial network in reproducing the measured data. A more refined evaluation of the results, particularly in the regions of the flow with a highly mixed laminar-turbulent structure, can be performed in the logarithmic domain. Of particular interest is the ability of this domain to represent exponential relationships as straight lines. This type of visual representation is provided in Figure 7. The figure confirms the superiority of the serial network model for this case, particularly in the region around $0.1 mm/s$. Here the serial network-based model offers excellent agreement with the measured data while the parallel network-based model shows significant deviation.

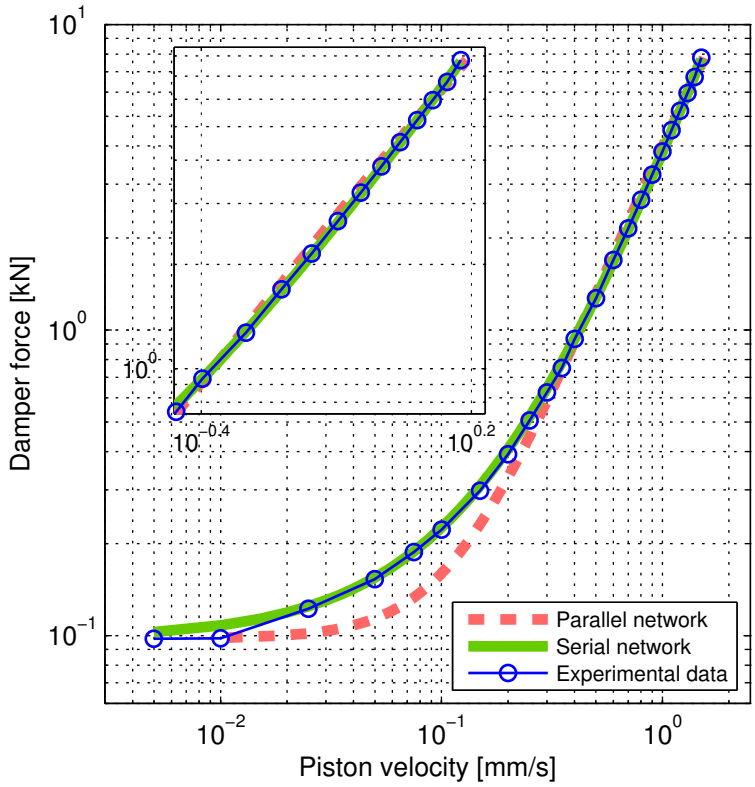

Figure 7 Comparison of identified parametric models with experimental data using logarithmic scales.

The presented results indicate a strong preference for the serial laminar-turbulent network model and they document its contribution to the pressure losses as identified with currently employed experimental methodology. This is in agreement with assumed nominal setup of the damper for given experimental conditions. Previous results also document that the serial laminar-turbulent model is adequate low-order representation of the flow patterns occurring in the range of studied piston velocities, i.e. the range of flow conditions induced by the piston movement.

4. CONCLUSIONS

The goal of current study was to perform structural analysis of the model of symmetric hydraulic damper based on the data provided by the novel experimental methodology

exploiting induced quasi-steady flow conditions in the damper. Resulting non-parametric estimates of the static characteristics were used with two alternative flow network models assuming incompressible flow conditions.

It was demonstrated in the current study that the serial flow network model is in better agreement with the experimental data than the model based on the parallel flow network model. This result is consistent with understanding of the nominal arrangement of the damper during tests. Further, the quality and consistency of the results provided by the serial flow network model suggests that this model is the adequate low-order choice for the modelling single-source mixed-flow pressure loss conditions.

ACKNOWLEDGMENTS

The authors gratefully acknowledge the support of the AgustaWestland.

REFERENCES

[1] B. Titurus, J. du Bois, N. Lieven, R. Hansford, A method for identification of the steady state characteristics of hydraulic dampers, Submitted to *Mechanical Systems and Signal Processing*, October 2009.

[2] R. Basso, Experimental characterisation of damping force in shock absorbers with constant velocity excitation, *Vehicle System Dynamics*, Vol. 30, No. 6, 1998, pp. 431–442.

[3] B. Titurus, N. Lieven, Modeling and analysis of active dampers in periodic working environments, *AIAA Journal*, Vol. 47, No. 10, October 2009, pp. 2404–2416.

[4] Bao M., Fu X., Chen Y., F. Scholl, Computational Fluid Dynamics approach to pressure loss analysis of hydraulic spool valve, *Fifth International Conference on Fluid Power Transmission and Control 2001*, Hangzhou, China, 3-5 April 2001.

[5] H. E. Merritt, *Hydraulic Control Systems*, John Wiley & Sons, New York, 1967.

[6] J. Wallaschek, Dynamics of non-linear automobile shock-absorbers, *International Journal of Non-Linear Mechanics*, Vol. 25, No. 2-3, 1990, pp. 299–308.

[7] C. Surace, K. Worden, G. R. Tomlinson, On the non-linear characteristics of automotive shock absorbers, *Proceedings of the Institution of Mechanical Engineers. Part D, Journal of automobile engineering*, Vol. 206, No. 1, 1992, pp. 3–16.

[8] M. D. Symans, M. C. Constantinou, Experimental testing and analytical modelling of semi-active fluid dampers for seismic protection, *Journal of Intelligent Material Systems and Structures*, Vol. 8, Number 8, August 1997, pp. 644–657.

[9] R. Van Kasteel, W. Cheng-Guo, Q. Lixin, L. Jin-Zhao, Y. Guo-Hong, A new shock absorber model for use in vehicle dynamics studies, *Vehicle System Dynamics*, Vol. 43, No. 9, September 2005, pp. 613–631.

[10] B. Yao, F. Bu, J. Reedy, G. T.-C. Chiu, Adaptive robust motion control of single-rod hydraulic actuators: Theory and experiments, *IEEE/ASME Transactions on Mechatronics*, Vol. 5, No. 1, March 2000, pp. 79–91.